

Influence of Anodizing Parameters on the Morphological Characteristics of TNTAs

Aamina¹, M.A. Hossen^{1,2}, A. Abd Aziz^{1*}

¹Faculty of Civil Engineering Technology, Universiti Malaysia Pahang Al-Sultan Abdullah, 26300 Kuantan, Pahang, Malaysia

²Center for Environmental Science and Engineering Research, Chittagong University of Engineering and Technology, Chattogram-4349, Bangladesh

ABSTRACT - TiO₂ nanotubes arrays (TNTAs) were synthesized using the anodization method in ethylene glycol (EG)-based electrolyte with different percentages of ammonium fluoride (0.3, 0.4, and 0.5 wt.%) and water content (2.5, 5, and 7.5% vol%). All the samples were ultrasonically cleaned in acetone, ethanol, and deionized water, then dried in air and kept in an etching solution for a while before anodization. The two-step anodization was carried out, followed by thermal treatment at 450°C for the crystallization. The nanotube samples were characterized using FE-SEM analysis. The FE-SEM results showed that the largest tube diameter was 87.74±1.89 nm of the TNTAs prepared in the EG electrolyte with a composition of 7.5% water content and 0.5% ammonium fluoride. The longest tube length analyzed was around 5.3 μm of the TNTAs prepared in the ethylene glycol electrolyte with the composition of 2.5% water content and 0.4% ammonium fluoride percentage, exhibiting a highly ordered, compact honeycomb structure and thick single-walled structure.

ARTICLE HISTORY

Received : 21st Sept. 2023

Revised : 03rd Oct. 2023

Accepted : 16th Oct. 2023

Published : 21st Dec. 2023

KEYWORDS

TNTAs

Anodization

Parameters

Morphology

Synthesis

1.0 INTRODUCTION

Titanium dioxide (TiO₂) is a widely studied photocatalyst with numerous applications, including solar cells, sensors, lithium-ion batteries [1, 2], medical implants [3–5], photocatalysis [6], and UV or sunlight-based water and air-cleaning properties [7]. This material's unique properties, such as its electrical, optical, and photocatalytic characteristics, high aspect ratio, and bioactivity, have significantly contributed. The electrochemical anodization method developed by Zwilling et al. in 1999 [8] using fluoride-containing electrolytes led to the self-organized growth of vertically oriented titanium dioxide nanotube arrays (TNTAs) on Ti alloy surfaces. This method has been extensively researched over the last few decades due to its low cost, ability to produce vertically oriented nanotube arrays directly on the substrate with good reproducibility, and optimization of TNTAs synthesis by different research groups.

Nanomaterials featuring morphologies from 0D to 3D are used to produce effective TiO₂ photocatalysts. In contrast, one-dimensional photocatalyst TNTAs display improved charge carrier separation in self-organized arrays, which results in outstanding photocatalytic characteristics. Based on these excellent qualities, Titania holds great promise in various fields of application [9]. The TNTA layers can be prepared by anodic oxidation of a Ti electrode in a fluoride-containing electrolyte. The variation in the electrolyte composition, fluoride concentration, water content, applied potential, and anodization time can be tuned to design a specific TNT length and wall thickness. In addition, extending one of these experimental parameters allows the TNTA morphology to be transformed into a porous nanostructure, exhibiting interesting photocatalytic properties. Indeed, increasing the anodization voltage makes it possible to form a porous sponge-like structure [10].

The enormous surface area and highly organized structures of TNTAs, which transfer electrons more rapidly than nanoparticles, make them a suitable material for anodes. Although ZnO, MgO, and CdS can be used to produce nanotubes, TiO₂ is preferred due to its nontoxicity, low cost, long-term chemical stability, highly ordered shape, promising optical and electrical properties, and one-dimensional direction of electron motions [11]. Several methods for TNTA synthesis have been developed, such as sol-gel, hydrothermal, solvothermal, and electrochemical anodization. Electrochemical anodization of the transition metal oxides has been majorly exploited over the past few decades due to the highly organized and vertically oriented mass production of nanotubes, alongside the swift process and least harmful for the environment among other industrially applicable methods [12]. The electric and optical behavior of anodic TNT strongly depends on its morphology, phase composition, and crystal facet arrangement. Modifying factors like voltage, anodization duration, and electrolyte composition also control nanotubes' architecture, such as diameters, nanotube length, and wall thickness. [13].

The functionalization of TiO₂ via nanostructuring renders it a leading application solution. Compared to other nanostructured materials, the high applicability of anodic TNTs is due to the vertical alignment of the structure that creates efficient transport channels while maximizing the reactive surface area. Moreover, the resulting geometry and structure

can be easily controlled and adjusted by modifying the anodization parameters, such as applied voltage, synthesis duration, and electrolyte composition [14].

In recent years, many scientists seemed to have been interested in TNT-enhanced morphology and engaged in publishing a plethora of papers on the individual effects of the synthesis parameters [10, 15–19]. However, the interaction effects of the variables are still a vast frontier to be explored and investigated. This study considers the influence of anodizing parameters such as electrolyte composition, fluoride content, and water content while keeping the applied potential and anodization duration constant to obtain the desired resulting morphology [20].

2.0 MATERIALS AND METHODS

2.1 Reagents and Materials

All the chemicals in this study were used as received from Sigma Aldrich Chemicals Company, used as analytical grade without further purification. To prepare TNTAs, titanium (Ti) foils with 0.127 mm thickness (99.97%) and graphite sheets cut into 20mm × 30mm sizes were used as anode and cathode, respectively. Ethylene glycol (EG, 99.5%), ammonium fluoride (NH₄F, 98.0%), and purified water from the Nanopure® water system prepared the electrolyte solutions. Ethyl alcohol (95%), acetone (99.5%), Hydrogen peroxide (99.5%), and purified water taken from the Nanopure® water system were utilized for all cleaning purposes before any experiment using ultrasonic cleaner (JAC-1020 P). A hotplate magnetic stirrer (HP-3000) was used for stirring the electrolyte throughout the anodization process. A DC Regulated Power Supply, High Precision Adjustable 5 Digit Programmable Henghui (PLD 21002, henghui), was employed for the anodization process. Finally, a muffle furnace (WiseTherm®, version 1.3.1) was employed for the annealing process.

2.2 Preparation of TNTAs

The TNTAs were prepared on top of 0.127 mm thick titanium foil (99.97 % pure). Ti foil was purchased from Sigma Aldrich Chemicals Company and cut into the desired 20mm × 30mm dimensions. Before the Anodization, the samples were ultrasonically cleaned in acetone (C₃H₆O), ethanol (C₂H₆O), and deionized water for 5 minutes, then dried in air. The cleaned samples were etched in a solution comprising HNO₃, HF, and DI water in a volume ratio of 1:1:3 to clean the surface from impurities before anodization. Two-step anodization was conducted in a two-electrode electrochemical cell with a graphite sheet as cathode and titanium foil as anode. The ethanol-based electrolyte was prepared using various amounts of ammonium fluoride (0.3%, 0.4%, 0.5%) and water content (2.5%, 5%, 7.5%). The prepared electrolyte was poured into a laboratory-scale beaker, and then the beaker was placed on a magnetic stirrer, as shown in Figure 1. The cathode and anode were held on a retort stand using a Pt-PTFE electrode holder to adjust the samples into the electrolyte. Control of voltages was adjusted by a DC Regulated Power Supply, High Precision Adjustable 5 Digit Programmable Henghui (PLD 21002, henghui). However, the voltage was kept constant at 40V for all the compositions. The anodization duration was also kept constant at 20 minutes for the first step and 1 hour for the second step anodization. The samples were ultrasonically cleaned after the 1st step of anodization to build up an anodic layer on the material's surface. After the 2nd step of Anodization, the samples were taken out, washed with deionized water, and dried in air. Hence, to get crystalline anatase TNTAs, the as-anodized sample was annealed in a programmable furnace for 2 h at 450°C.

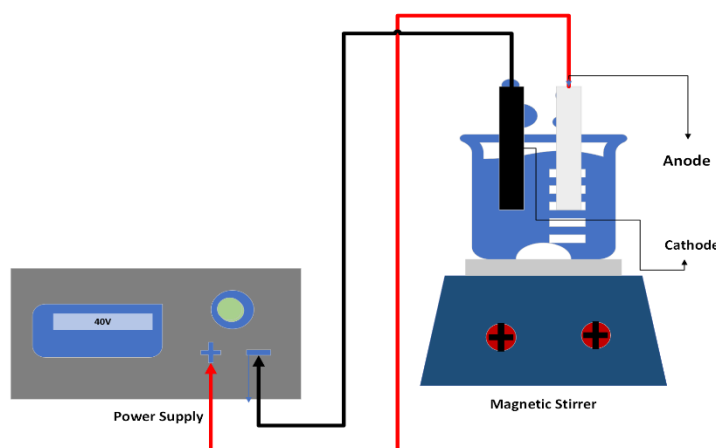


Figure 1. Schematic illustration of the electrochemical anodization setup

2.3 Characterization of Prepared TNTAs

The morphological characterization of the prepared TNTs was analyzed by a Field Emission Scanning Electron Microscope (FESEM) JEOL (JSM-7600F) at the Centre of Excellence for Advanced Research in Fluid Flow (CARRIF) Universiti Malaysia Pahang (UMP). The equipment was furnished with an energy-dispersive X-ray spectroscopy (EDX) for elemental analysis. To produce the analysis images, a 5.0 kV accelerating voltage was applied.

3.0 EXPERIMENTAL RESULTS

This experiment investigates the morphological characteristics of the prepared TNTAs and the influence of the changing anodization parameters. Voltage and Anodization time were kept constant to study the effect of ammonium fluoride percentage and water content in the composition of Ethylene Glycol electrolyte. Three distinct water content (2.5%, 5% and 7.5%) and ammonium fluoride percentages (0.3%, 0.4% and 0.5%) were utilized. The microstructure of the TNTAs after anodic oxidation in Ethylene Glycol at 40V was characterized based on the FE-SEM images obtained, as shown in Figure 1 – Figure 9. All the FE-SEM images were analyzed using the ImageJ software, and the results were plotted as a histogram with a distribution curve using the Origin Pro software. Based on the FE-SEM images and the analysis, it can be concluded that the higher percentage of water content in combination with higher ammonium fluoride gave the larger diameter; however, the tube length remained the shortest.

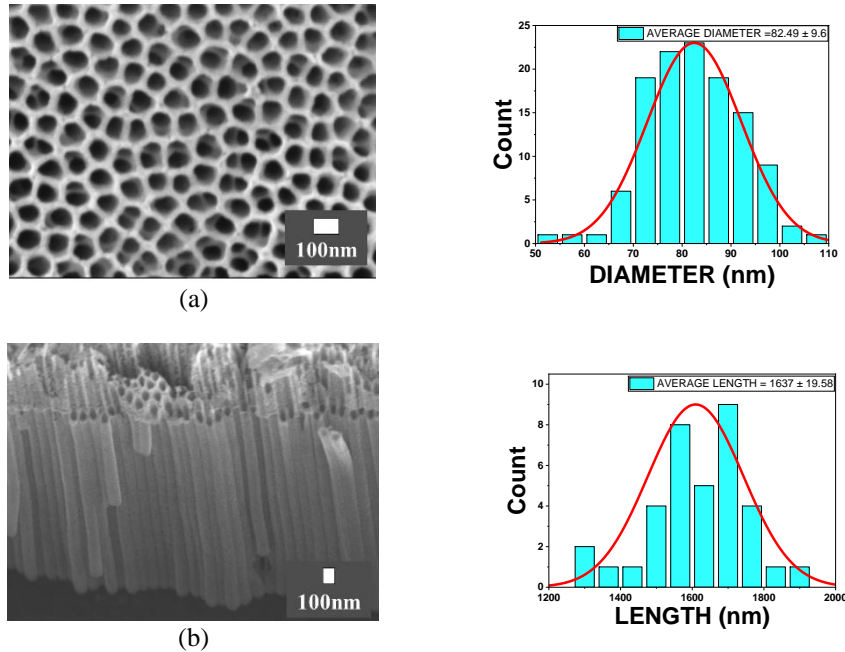


Figure 2. FESEM analysis and histogram with distribution diagram of prepared TNT (2.5% H₂O content and 0.3% NH₄F concentration) (a) Top view and (b) Cross-sectional view

Figure 2 shows the surface morphology of the anodized TNTAs in the ethylene glycol electrolyte with 2.5% H₂O and 0.3 wt.% NH₄F concentration. FE-SEM images show the distinct morphological features resulting from the variation of the synthesis parameters. Interestingly, this lower ammonium fluoride percentage exhibited a larger pore diameter of 82.49±9.6, while the growth of nanotube length was limited to 1.6 ±0.19µm due to lower Fluoride ions. However, the morphology obtained is similar to the study, adopting almost the same parameters [21]. The surface morphology of the TNTAs exhibits a highly ordered, aligned, and homogenous surface structure of TNTAs.

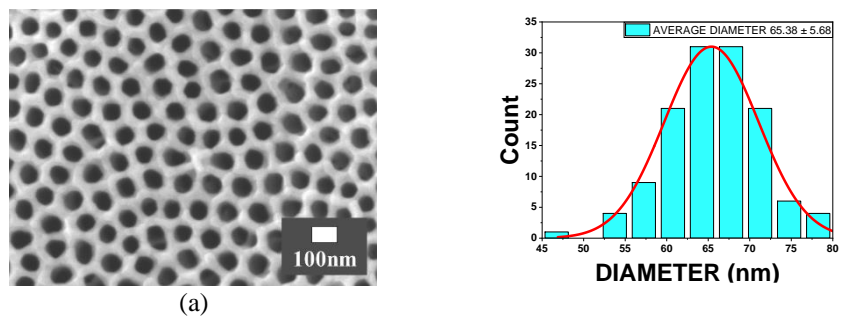
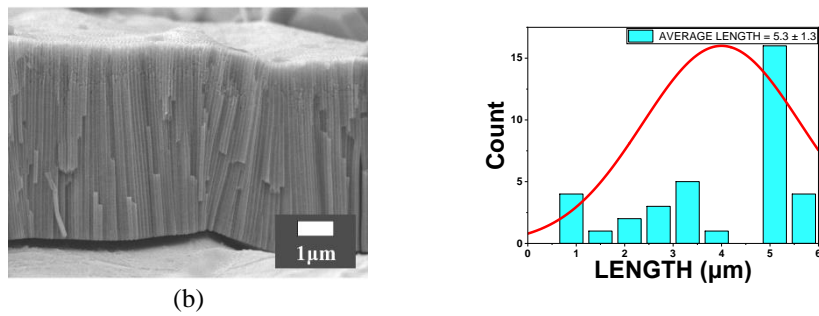


Figure 3. FESEM analysis and histogram with distribution diagram of prepared TNT (2.5% H₂O content and 0.4% NH₄F concentration) (a) Top view



(b) Figure 3. (cont.) (b) Cross-sectional view

Figure 3 shows the surface morphology of the anodized TNTAs in the ethylene glycol electrolyte with 2.5% H₂O and 0.4 wt.% NH₄F concentration. However, each FE-SEM image shows distinct morphological features resulting from every single variation of the synthesis parameters. Interestingly, this composition of ammonium fluoride percentage exhibited a pore diameter ranging from 65.38±5.68 nm while attaining the highest growth of nanotube length 5.3±1.3 μm. The surface morphology of the TNTAs exhibits a highly ordered, aligned, and homogenous surface structure of TNTAs. As seen in the FE-SEM images, the structure contains a honeycomb-like homogenous surface structure. The morphological characteristics obtained in this study are consistent with the previous study conducted by Liang and coworkers [21].

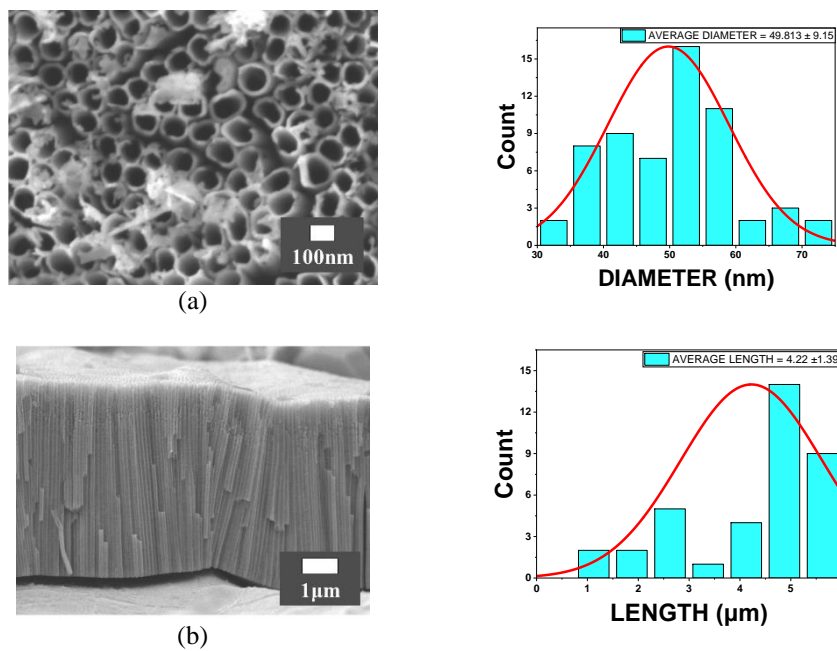


Figure 4. FESEM analysis and histogram with distribution diagram of prepared TNT (2.5% H₂O content and 0.5% NH₄F concentration) (a) Top view and (b) Cross-sectional view

Figure 4 shows the surface morphology of the anodized TNTAs in the ethylene glycol electrolyte with 2.5% H₂O and 0.5 wt.% NH₄F concentration. However, this composition of ammonium fluoride percentage exhibited a pore diameter ranging from 49.813±9.15 nm, with an average growth of nanotube length of 4.22±1.3 μm found, which is similar to other TNTA films synthesized under similar conditions reported in the literature [22]. The surface morphology of the TNTAs exhibits the inhomogeneous surface structure of TNTAs. As seen in the FE-SEM images, the structure contains longer nanotubes, but the porous structure contains some debris over the nanotubes. Excess fluoride ions lead to chemical etching and thinning of the walls of the pores, which resulted in the demolition of nanotube structures.

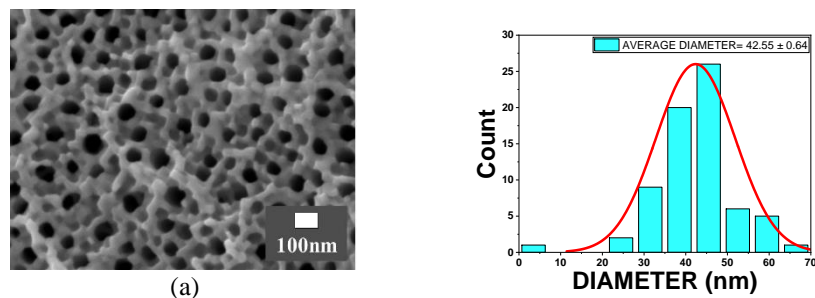
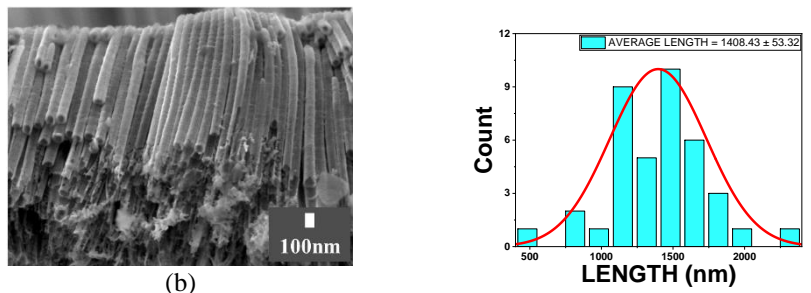


Figure 5. FESEM analysis and histogram with distribution diagram of prepared TNT (5% H₂O content and 0.3% NH₄F concentration) (a) Top view



(b) Figure 5. (cont.) (b) Cross-sectional view

Figure 5 shows the surface morphology of the anodized TNTAs in the ethylene glycol electrolyte with 5% H₂O and 0.3 wt.% NH₄F concentration. As seen in the images, this electrolyte composition exhibits the unique structure of the TNTAs. The nanotube length is bent and fallen as the structure of the TNTAs starts to grow, as the chemical etching begins to grow the oxide layer. The porous structure also shows that the top layer of TNTAs is destroyed, and the remaining debris covers the pore diameter. However, this composition of ammonium fluoride percentage exhibited a pore diameter ranging from 42.55±0.64 nm, with an average growth of nanotube length 1.4±0.53 μm. The surface morphology of the TNTAs exhibits the inhomogeneous surface structure of TNTAs, which is similar to a previous study [23].

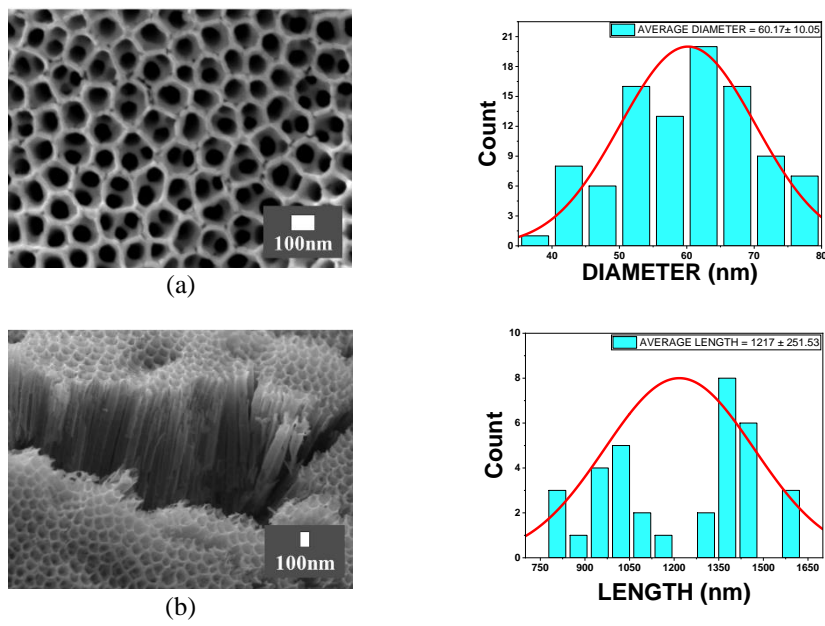


Figure 6. FESEM analysis and histogram with distribution diagram of prepared TNT (5% H₂O content and 0.4% NH₄F concentration) (a) Top view and (b) Cross-sectional view

Figure 6 analyses the surface morphology of the anodized TNTAs in the ethylene glycol electrolyte with 5% H₂O and 0.4 wt.% NH₄F concentration. As discussed earlier, the fluoride ions migrate to the walls of the pore during formation, and the water content in the electrolyte allows chemical etching, resulting in the thinning of the tube walls. This phenomenon will result in the development and dissolution of nanotube arrays, as observed in previous studies [24]. As shown in Figure 6(a), the upper surface lost the thin walls of a few nanotubes, and the inner two three porous structures can be seen through it. However, this composition of ammonium fluoride percentage exhibited a pore diameter ranging from 60.17±10.05 nm, with an average growth of nanotube length 1.17±0.25 μm. The surface morphology of the TNTAs exhibits the homogenous surface structure of TNTAs.

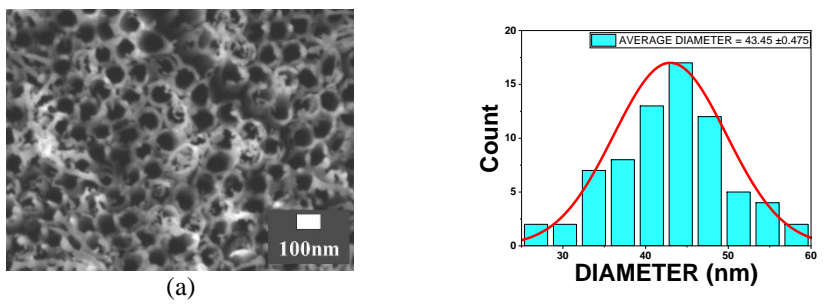
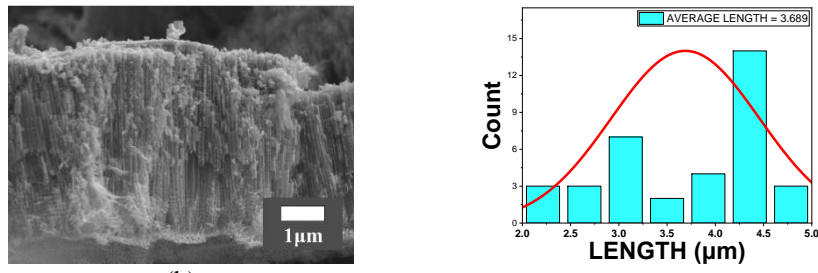


Figure 7. FESEM analysis and histogram with distribution diagram of prepared TNT (5% H₂O content and 0.5% NH₄F concentration) (a) Top view



(b)
Figure 7. (cont.) (b) Cross-sectional view

Figure 7 analyses the surface morphology of the anodized TNTAs in the ethylene glycol electrolyte with 5% H₂O and 0.5 wt.% NH₄F concentration. As discussed earlier, excess chemical etching results in the thinning of nanotube walls due to the increased fluoride ions accumulation inside pores and its chemical etching. As seen in Figures 7(a) and 7(b), the debris accumulated over the top and sides of the nanotubes destroys the homogenous structure of the tubes. However, this composition of ammonium fluoride percentage exhibited a pore diameter ranging from 43.45±0.475 nm, with an average growth of nanotube length 3.689 μm. The surface morphology of the TNTAs exhibits the inhomogeneous surface structure of TNTAs and is in line with the structure attained in previous studies [23].

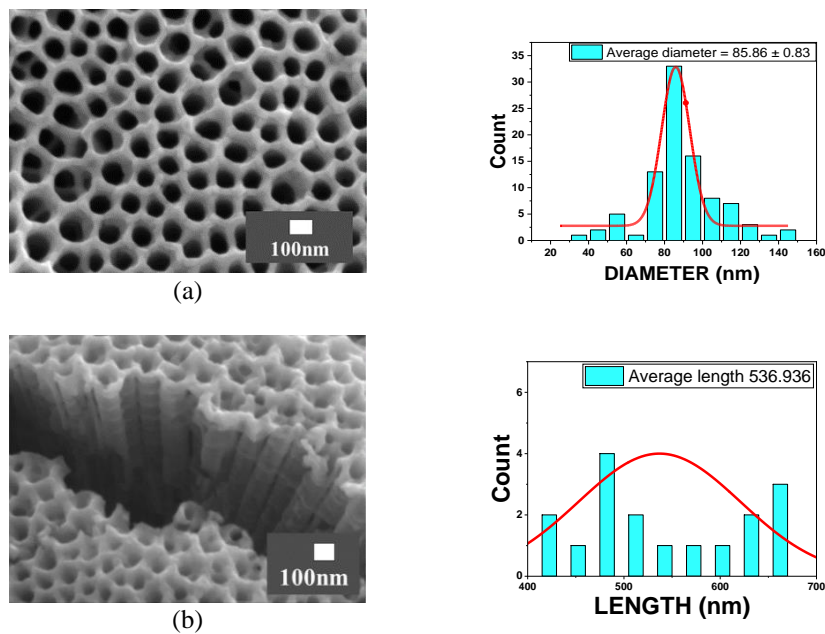


Figure 8. FESEM analysis and histogram with distribution diagram of prepared TNT (7.5% H₂O content and 0.3% NH₄F concentration) (a) Top view and (b) Cross-sectional view

Figure 8 shows the surface morphology of the anodized TNTAs in the ethylene glycol electrolyte with 7.5% H₂O and 0.3 wt.% NH₄F concentration. As seen in Figures 8(a) and 8(b), the homogeneity of the structure of the TNTAs is consistent and concise. However, this composition of ammonium fluoride percentage exhibited the second highest pore diameter, ranging from 85.86±0.83 nm as observed in the previous study [21], with an average growth of nanotube length of 0.536μm. The surface morphology of the TNTAs exhibits the homogenous surface structure of TNTAs. As observed, the low fluoride ions presence hindered the growth of nanotubes, but they resisted the excess chemical etching and loss of structure of nanotubes, resulting in homogenous semi-honeycomb structures.

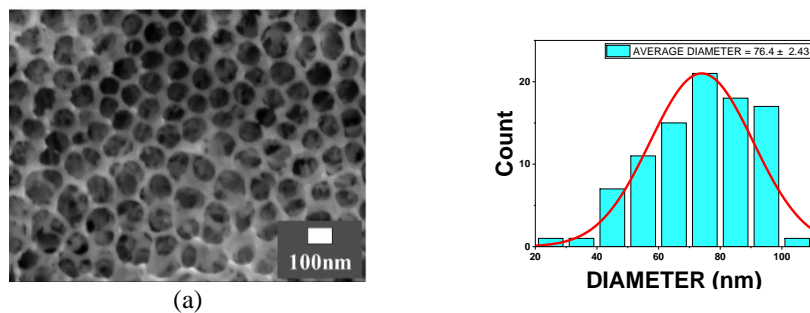


Figure 9. FESEM analysis and histogram diagram of prepared TNT (7.5% H₂O content and 0.4% NH₄F concentration) (a) Top view and

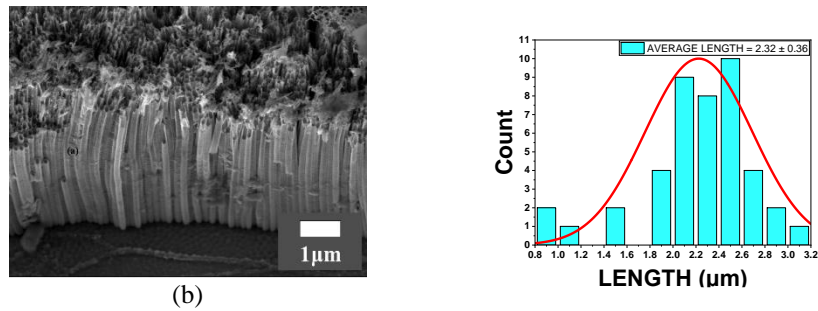


Figure 9. (cont.) (b) Cross-sectional view

Figure 9 shows the surface morphology of the anodized TNTAs in the ethylene glycol electrolyte with 7.5% H₂O and 0.4 wt.% NH₄F concentration. As seen in Figures 9(a) and 9(b), the homogeneity of the TNTAs' structure is inconsistent. The top layer of the nanotube is bent on one side; the porous structure of the nanotube is inconsistent, and the walls are thin. However, this composition of ammonium fluoride percentage exhibited a pore diameter ranging from 76.4±2.43nm, with an average growth of nanotube length 2.32±0.36 μm. The surface morphology of the TNTAs shows the enormous growth of nanostructure tubes and diameter, but at some point, it started to destroy both the tube length and diameter. This shift might lead to a change in the development of the oxide layer and, ultimately, to its dissolution. A similar phenomenon was observed recently for growing nanoporous arrays in previous studies [23].

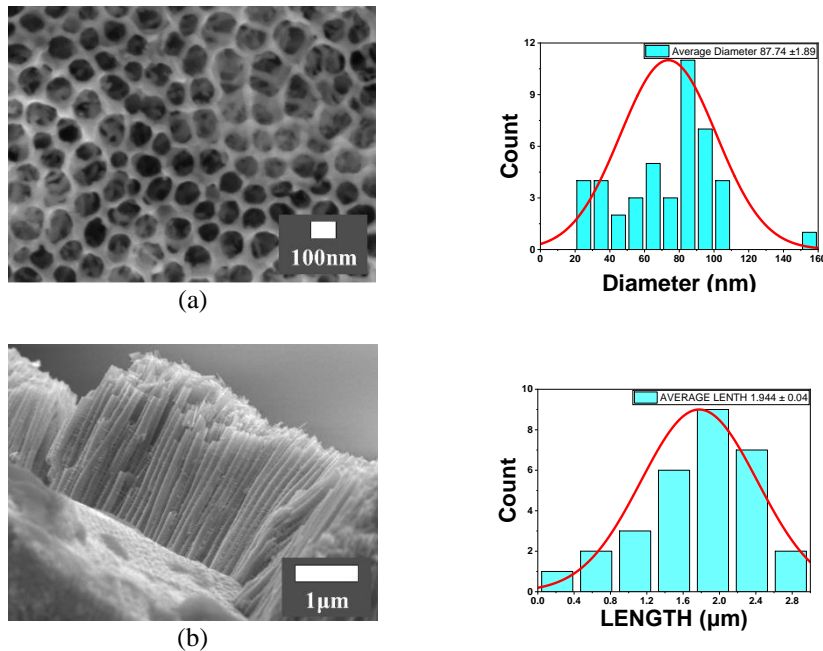
Figure 10. FESEM analysis and histogram diagram of prepared TNT (7.5% H₂O content and 0.5% NH₄F concentration) (a) Top view and (b) Cross-sectional view

Figure 10 shows the surface morphology of the anodized TNTAs in the ethylene glycol electrolyte with 7.5% H₂O and 0.4 wt.% NH₄F concentration. As seen in Figures 10(a) and 10(b), the homogeneity of the top structure of the TNTAs is inconsistent. Due to the excess chemical etching, the nanotube walls are thinner. At the same time, the compactness of the nanotube length shows enormous growth and homogeneity. However, this composition of ammonium fluoride percentage exhibited the highest pore diameter, ranging within 87.74±1.89 nm, with an average growth of nanotube length 1.944±0.04 μm. The surface morphology of the TNTAs exhibits the enormous growth of nanostructure tubes and diameter, as described in a previous study conducted by Ribeiro and his coworkers [23]. Detailed research regarding the parameter is listed in Table 2, depicting the changes in the morphology of the prepared TNTAs and the influence of anodizing parameters.

The chemical composition and purity of TiO₂ nanotube array samples were investigated using EDX analysis, as presented in Table 1. Only peaks belonging to Ti and O elements were found in the EDX spectrum of the TNT sample, with no signs of any impurities other than C, which is due to the annealing being applied to the sample for crystallization. Table 1 shows the EDX analysis of porous TiO₂ nanostructures obtained by anodization in 2.5% H₂O 0.4wt% NH₄F at 40V for one hour, followed by annealing. The calculated atomic ratio for porous TiO₂ nanotubes is (32.60±0.73%) and oxygen (63.17±1.01%). In our substrate, the weight percent for Ti and O is 59.53±1.34% and 38.53±0.61%, respectively. It is confirmed that the atomic ratio of titanium to oxygen is 1:2 (well-matching TiO₂). Moreover, we can observe a peak corresponding to C remaining in the TiO₂ nanostructures of electrolyte, and its wt% is almost 1.

Table 1. EDX semi-quantitative analysis of TNTA films produced from Ti Foil anodization in Ethylene glycol (2.5% H₂O content and 0.4% NH₄F concentration)

Element	Mass%	Atom %
C	1.94±0.06	4.23±0.12
O	38.53±0.61	63.17±1.01
Ti	59.53±1.34	32.60±0.73

3.1 Parametric study

This experiment investigates the morphological characteristics of the prepared TNTAs and the influence of the changing anodization parameters. Voltage and anodization time were kept constant to study the effect of ammonium fluoride percentage and water content in the composition of the third-generation EG electrolyte. Three distinct water content (2.5%, 5%, and 7.5%) and ammonium fluoride percentages (0.3%, 0.4%, and 0.5%) were set up and the samples were prepared independently. The prepared samples were annealed to get the amorphous crystalline structure of the TNTAs. The parametric study of the prepared sample is tabulated below.

Table 2. Comparison of ethanol-based electrolytes prepared TNTAs morphology at various ammonium fluoride and water content (constant anodization time and voltage)

Electrolyte	H ₂ O (%)	NH ₄ F (%)	Tube length (μm)	Tube diameter (nm)	Time	Voltage
Ethylene Glycol (EG)	2.5%	0.3%	1.6 ±0.19	82.49±9.6	1st step 20 minutes 2nd step 1 h	40V
		0.4%	5.3±1.3	65.38±5.68		
		0.5%	4.22±1.3	49.813±9.15		
	5%	0.3%	1.4±0.53	42.55±0.64		
		0.4%	1.17±0.25	60.17±10.05		
		0.5%	3.689	43.45±0.475		
	7.5%	0.3%	0.536	85.86±0.83		
		0.4%	2.32±0.36	76.4±2.43		
		0.5%	1.944±0.04	87.74±1.89		

The ammonium fluoride percentage added to the electrolyte influences the nanotube diameter formation and the arrays' length. Figures 11 and 12 present the relationship among nanotube diameter, length, and concentration of NH₄F. The ammonium fluoride percentage showed different effects on the length and nanotube diameter depending on the water content. The 0.3 wt.% NH₄F and 0.5% wt.% NH₄F with combination of 5% of H₂O exhibited the lowest diameter. However, the tube diameter increased to 87.74±1.89 when the Anodization was carried out with an electrolyte containing 0.5% wt. % NH₄F and 7.5% water content. However, the higher percentage of NH₄F reduced the length, which can be caused by the drastic chemical dissolution due to the increased number of fluoride ions on the surface of TNTAs. Whereas the diameter of the TNTAs exhibited a marginal increase with the increase in NH₄F content [25]. During the anodization process, the growth of oxide thickness is due to the ion migration across the anodic film. The fluoride ions are the fastest inward moving ions than any other ions, forming a fluoride-rich layer (FRL) on the Ti- interface. The scallop-shaped bottom of the nanotubes shows that the FRL is the inter-pore material, indicating a flow mechanism in the oxide pore formation. When the FRL is dissolved by water, pores are separated, resulting in discrete nanotubes. The large amount of FRL sticks around the walls of the nanotube pores, the water content in the electrolyte results in excess dissolution of this FRL, and the TNTAs are formed with thin walls [26]. As seen in the FE-SEM images, all the TNTAs prepared in the electrolyte containing 0.5 wt.% NH₄F had thinner walls and an inhomogeneous surface structure. Considering this, the electrolyte with the 0.4 wt.% NH₄F concentration was considered optimum due to the adequate surface etching and considerable length of the TNTAs.

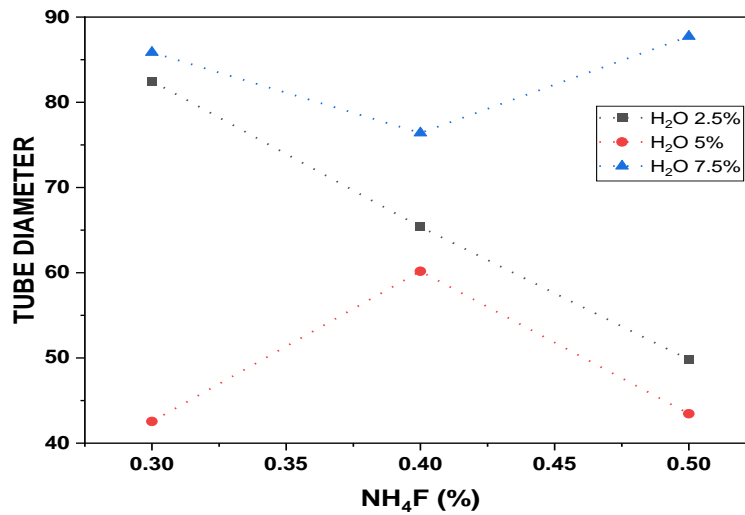


Figure 11. Relationship between nanotube diameter and concentration of NH_4F (wt.%)

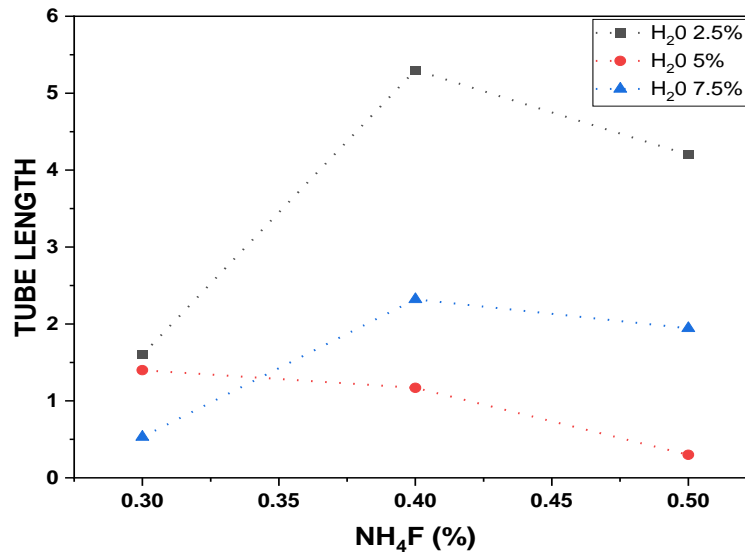


Figure 12. Relationship between nanotube length and concentration of NH_4F (wt.%)

4.0 CONCLUSION

The present study was conducted to optimize anodizing parameters for the optimum morphology of Titanium dioxide Nanotube Arrays. To study the influence of the anodizing parameters, the amount of ammonium fluoride and water content was varied while keeping the rest constant. However, the highest pore diameter of 87.74 ± 1.89 nm was formed from the TNTAs prepared in the composition of Ethylene Glycol with 7.5% water and 0.5% NH_4F . The most homogenous, well-aligned, and honeycomb structure was obtained from the TNTA samples prepared in the ethylene glycol electrolyte with 2.5% water content and 0.4% NH_4F concentration. The sample exhibited a pore diameter ranging from 65.38 ± 5.68 nm while attaining the highest growth of nanotube length 5.3 ± 1.3 μm . The surface morphology of the TNTAs exhibits a highly ordered, aligned, and homogenous surface structure of TNTAs. As seen in the FE-SEM images, the structure contains a honeycomb-like homogenous surface structure. It was observed that the ammonium fluoride and water content influenced the morphological characteristics of the TNTAs simultaneously.

5.0 AUTHOR CONTRIBUTIONS

Aamina: Conceptualization, Methodology, Software, Writing- Original Draft Preparation

Md. Arif Hossen: Conceptualization, Methodology, Writing- Reviewing and Editing

Azrina Abd Aziz: Supervision, Writing- Reviewing and Editing

6.0 FUNDING

The support provided by Universiti Malaysia Pahang in the form of a research grant vote number Distinguished Research Grant RDU223005 for this study is highly appreciated.

7.0 DATA AVAILABILITY STATEMENT

The data used to support the findings of this study are included within the article.

8.0 ACKNOWLEDGEMENT

The authors would like to thank the Faculty of Civil Engineering Technology for providing the experimental facilities and to all technicians at Environmental Engineering Laboratory.

9.0 CONFLICTS OF INTEREST

The authors declare no conflict of interest.

10.0 REFERENCES

- [1] W. Cao, K. Chen, and D. Xue, "Highly ordered TiO₂ nanotube arrays with engineered electrochemical energy storage performances," *Materials (Basel)*, vol. 14, no. 3, pp. 1–12, 2021.
- [2] M. M. Muzakir, Z. Zainal, H. N. Lim, A. H. Abdullah, N. N. Bahrudin, and M. S. M. Ali, "Electrochemically reduced titania nanotube synthesized from glycerol-based electrolyte as supercapacitor electrode," *Energies*, vol. 13, no. 11, pp. 2767, 2020.
- [3] B. Łosiewicz, A.S. Stróż, P. Osak, J. Maszybrocka, A. Gerle, K. Dudek *et al.*, "Production, characterization and application of oxide nanotubes on Ti–6Al–7Nb alloy as a potential drug carrier," *Materials (Basel)*, vol. 14, no. 20, pp. 6142, 2021.
- [4] J. Rios, V.N. Santini, K.D. Pereira, A.D. Luchessi, É.S.N. Lopes, R. Caram *et al.*, "Self-organized TiO₂ nanotubes on Ti-Nb-Fe alloys for biomedical applications: Synthesis and characterization," *Electrochemistry Communications*, vol. 138, pp.107280, 2022.
- [5] K. A. Kravanja, L. Suhadolnik, M. Bele, U. Maver, J. Rožanc, Ž. Knez *et al.*, "The synthesis, surface analysis, and cellular response of titania and titanium oxynitride nanotube arrays prepared on TiAl6V4 for potential biomedical applications," *Journal of Materials Research and Technology*, vol. 24, pp. 4074–4090, 2023.
- [6] T.J. Awaid, A.K. Ayal, A.M. Farhan, M.S. Sando, and L.Y. Chin, "Effect of electrolyte composition on structural and photoelectrochemical properties of titanium dioxide nanotube arrays synthesized by anodization technique," *Baghdad Science Journal*, vol. 17, no. 4, pp. 1183–1190, 2020.
- [7] Y. Wang, X. Zhang, S. You, and Y. Hu, "One-step electrosynthesis of visible light responsive double-walled alloy titanium dioxide nanotube arrays for use in photocatalytic degradation of dibutyl phthalate," *RSC Advances*, vol. 10, no. 36, pp. 21238–21247, 2020.
- [8] V. Zwilling, M. Aucoeur, and E. Darque-Ceretti, "Anodic oxidation of titanium and TA6V alloy in chromic media. An electrochemical approach," *Electrochimica Acta*, vol. 45, no. 6, pp. 921–929, 1999.
- [9] M.L. Puga, J. Venturini, C.S. ten Caten, and C.P. Bergmann, "Influencing parameters in the electrochemical anodization of TiO₂ nanotubes: Systematic review and meta-analysis," *Ceramics International*, vol. 48, no. 14, pp. 19513–19526, Jul. 2022.
- [10] M.A. Hossen, N. Yaacof, A.A. Aziz, and W. Lihua, "Latest progress on the influencing factors affecting the formation of TiO₂ nanotubes (TNTs) in electrochemical anodization- A minireview," *Acta Chemica Malaysia*, vol. 7, no. 1, pp. 8–15, 2023.
- [11] Misriyani and E. S. Kunarti, "Synthesis and photoelectrochemical activity of TiO₂ nanotube based free standing membrane," *Asian Journal of Chemistry*, vol. 32, no. 11, pp. 2739–2742, 2020.
- [12] M.A. Hossen, H.M. Solayman, K.H. Leong, L.C. Sim, N. Yaacof, A.A. Aziz, and W. Lihua, "A Comprehensive Review on Advances in TiO₂ Nanotube (TNT)-Based Photocatalytic CO₂ Reduction to Value-Added Products," *Energies*, vol. 15, no. 22, pp. 8751, 2022.
- [13] X. Hou, P. D. Lund, and Y. Li, "Controlling anodization time to monitor film thickness, phase composition and crystal orientation during anodic growth of TiO₂ nanotubes," *Electrochemistry Communications*, vol. 134, pp. 107168, 2022.
- [14] P. Nakpan and A. Aeimbhu, "Fabrication of titanium dioxide nanotubes by difference the anodization voltage and time," *Materials Today: Proceedings*, vol. 47, pp. 3436–3440, 2021.

- [15] M. Michalska-Domańska, M. Czerwiński, M. Łazińska, V. Dubey, M. Jakubaszek, Z. Zawadzki, and J. Kostecki, "Morphological and optical characterization of colored nanotubular anodic titanium oxide made in an ethanol-based electrolyte," *Materials (Basel)*, vol. 14, no. 22, pp. 6992, 2021.
- [16] B. Ribeiro, R. Offoiaich, E. Rahimi, E. Salatin, M. Lekka, and L. Fedrizzi, "On Growth and morphology of TiO₂ nanotubes on Ti6Al4V by anodic oxidation in ethylene glycol electrolyte: Influence of microstructure and anodization parameters," *Materials*, vol. 14, no. 10, p. 2540, May 2021.
- [17] M.A. Hossen, F. Khatun, R.R. Ikreedeegh, A.D. Muhammad, A.A. Aziz, K.H. Leong, "Enhanced photocatalytic CO₂ reduction to CH₄ using novel ternary photocatalyst RGO/Au-TNTAs," *Energies*, vol. 16, no. 14, pp. 5404, 2023.
- [18] M.A. Hossen, H.M. Solayman, K.H. Leong, L.C. Sim, N. Yaacof, A.A. Aziz *et al.*, "Recent progress in TiO₂-Based photocatalysts for conversion of CO₂ to hydrocarbon fuels: A systematic review," *Results in Engineering*, vol. 16, pp. 100795, 2022.
- [19] N. T. Van Anh, M. T. Xuan, P. T. Binh, and M. T. T. Thuy, "Investigation of photoelectrochemical properties of TiO₂ nanotube arrays prepared by anodization method," *Vietnam Journal of Chemistry*, vol. 58, no. 2, pp. 180–184, 2020.
- [20] H. Ennaceri, K. Fischer, K. Hanus, A. Chemseddine, A. Prager, J. Griebel *et al.*, "Effect of morphology on the photoelectrochemical activity of TiO₂ self-organized nanotube arrays," *Catalysts*, vol. 10, no. 3, pp. 1–15, 2020.
- [21] L. Hao, S. Tang, J. Yan, L. Cheng, S. Guan, Q. Zhao *et al.*, "Solar-responsive photocatalytic activity of amorphous TiO₂ nanotube-array films," *Materials Science in Semiconductor Processing*, vol. 89, no. 1038, pp. 161–169, 2019.
- [22] J. S. Santos, M. Fereidooni, V. Marquez, M. Arumugam, M. Tahir, S. Prasertthdam *et al.*, "Single-step fabrication of highly stable amorphous TiO₂ nanotubes arrays (am-TNTA) for stimulating gas-phase photoreduction of CO₂ to methane," *Chemosphere*, vol. 289, pp. 133170, 2022.
- [23] B. Ribeiro, R. Offoiaich, S. Rossetti, E. Salatin, M. Lekka, and L. Fedrizzi, "On growth and morphology of TiO₂ nanotubes on CP-Ti by anodic oxidation in ethylene glycol electrolyte: Influence of electrolyte aging and anodization parameters," *Materials (Basel)*, vol. 15, no. 9, pp. 3338, 2022.
- [24] Y.V. Yuferov, I.D. Popov, F.M. Zykov, A.Y. Suntsov, I.V. Baklanova, A.V. Chukin *et al.*, "Study of the influence of anodizing parameters on the photocatalytic activity of preferred oriented TiO₂ nanotubes self-doped by carbon," *Appl. Surf. Sci.*, vol. 573, pp. 151366, 2022.
- [25] M.I. Broens, W.R. Cervantes, D. Oyarzún Jerez, M.L. Tejjelo, and O.E. Linarez Pérez, "The keys to avoid undesired structural defects in nanotubular TiO₂ films prepared by electrochemical anodization," *Ceramics International*, vol. 46, no. 9, pp. 13599–13606, 2020.
- [26] S.A. Rosli, N. Alias, N. Bashrom, S. Ismail, W.K. Tan, G. Kawamura *et al.*, "Hexavalent chromium removal via photoreduction by sunlight on titanium-dioxide nanotubes formed by anodization with a fluorinated glycerol-water electrolyte," *Catalysts*, vol. 11, no. 3, pp. 1–19, 2021.